Title: MmpL3 is the flippase for mycolic acids in mycobacteria

Authors: Zhujun Xu[a], Giovanna Poce[c], Shu-Sin Chng[a,b,*]

Affiliations:

[a]Department of Chemistry, National University of Singapore, Singapore 117543.

[b]Singapore Center on Environmental Life Sciences Engineering (SCELSE), National University of Singapore, Singapore 117456.

[c]Dipartimento di Chimica e Tecnologie del Farmaco, Sapienza University of Rome, Rome 00185, Italy

[*]To whom correspondence should be addressed. E-mail: chmchngs@nus.edu.sg

Author contributions: Z.X. and S.-S.C. designed research; Z.X. performed all experiments described in this work; G.P. synthesized and provided BM212; Z.X., and S.-S.C. analyzed and discussed data; Z.X., and S.-S.C. wrote the paper.

The authors declare no conflict of interest.

Classification

Biological Sciences - Biochemistry

Abstract

The defining feature of the mycobacterial outer membrane (OM) is the presence of mycolic acids (MAs), which in part render the bilayer extremely hydrophobic and impermeable to external insults, including many antibiotics. While the biosynthetic pathway of MAs is well studied, the mechanism(s) by which these lipids are transported across the cell envelope is(are) much less known. MmpL3, an essential inner membrane (IM) protein, is implicated in MA transport, but its exact function has not been elucidated. It is believed to be the cellular target of several anti-mycobacterial compounds; however, evidence for direct inhibition of MmpL3 activity is also lacking. Here, we establish that MmpL3 is the MA flippase at the IM of mycobacteria, and show that a 1,5-diarylpyrrole compound, BM212, directly inhibits this activity. We develop assays that selectively access mycolates on the surface of *Mycobacterium smegmatis* spheroplasts, allowing us to monitor flipping of MAs across the IM. Using these assays, we establish the mechanism-of-action of BM212 as an MmpL3 inhibitor, and employ it as a molecular probe to demonstrate the requirement of functional MmpL3 for the transport of MAs across the IM. Our work provides fundamental insights into OM biogenesis and MA transport in mycobacteria. Furthermore, our assays serve as an important platform for accelerating the validation of small molecules that target MmpL3, and their development as future anti-tuberculosis drugs.

Keywords

Mycobacterium tuberculosis; membrane biogenesis; lipid transport; trehalose monomycolate; Mycobacterial membrane protein Large; Resistance, Nodulation, and Cell Division

Significance statement

Biological membranes define cellular boundaries, allow compartmentalization, and represent a prerequisite for life; yet, our understanding of membrane biogenesis remains rudimentary. Mycobacteria, including the human pathogen *Mycobacterium tuberculosis*, are surrounded by a double-membrane cell envelope that makes them intrinsically resistant to many antibiotics. Specifically, the outer membrane contains unique lipids called mycolic acids, whose transport mechanism across the envelope is unknown. In this study, we established the role of an essential membrane protein as the flippase for mycolic acids, and demonstrated that this protein is a target of putative anti-tuberculosis compounds. Our work provides insights into outer membrane biogenesis and lipid transport in mycobacteria, and also the means to evaluate drugs that disrupt mycolic acid transport at the inner membrane.

Introduction

The outer membrane (OM) of *Mycobacterium tuberculosis*, the causative agent of tuberculosis (TB), is distinctively characterized by the abundance of mycolic acids (MAs), C_{60}-C_{90} long chain, branched fatty acids, packed together to produce a bilayer with markedly reduced fluidity and permeability (Brennan & Nikaido, The envelope of mycobacteria, 1995). These MAs come in the forms of trehalose monomycolates (TMMs), trehalose dimycolates (TDMs), and mycolates covalently attached to arabinogalactan (AG) polysaccharides, which are in turn linked to the peptidoglycan and collectively known as the mAGP complex (Fig. 1*A*). MAs are synthesized at the inner membrane (IM) as TMMs via a highly-conserved and well-characterized pathway (2), which is the target of first line anti-TB drug, isoniazid (3). How MAs are transported across the cell envelope and assembled into the OM, however, is less understood; proteins mediating TMM flipping across the IM and transit across the periplasm have not been identified and/or characterized (Fig. 1*A*). At the OM, the Ag85 complex transfers a mycolate chain from one TMM molecule to another to form TDM, or to the AG polysaccharides to form the mAGP complex (4). Tethering the OM to the cell wall via the AG polysaccharides further rigidifies the membrane, making it extremely impermeable to a wide range of compounds, including many antibiotics (1). The OM, and hence MAs, are essential for mycobacterial growth.

Recently, a conserved essential IM protein, MmpL3 (Mycobacterial membrane protein Large 3), has been implicated in MA transport. Depletion of *mmpL3* in *Mycobacterium smegmatis* results in accumulation of TMMs and reduced formation of TDMs and AG-linked mycolates (5,6), suggesting an impairment in TMM transport to the OM. Consistent with this,

MmpL3, like other MmpL proteins, belongs to the resistance, nodulation, and cell division (RND) protein superfamily, and is believed to be a proton motive force (pmf)-dependent transporter (7). Based on its cellular localization, MmpL3 is likely involved in either TMM flipping across the IM, TMM release from the IM into the periplasm, or both (Fig. 1*A*). Yet, its exact role has not been clearly defined, due largely to the lack of functional assays for its putative transport activity. Treatment of mycobacteria with a few structurally-distinct small molecule scaffolds, including ethylenediamines (e.g. SQ109) (8), 1,5-diarylpyrroles (e.g. BM212) (9,10), adamantyl ureas (e.g. AU1235) (5), and others (11,12,13,14,15), result in similar changes in mycolate species as in *mmpL3* depletion. These compounds inhibit growth, and select for resistance mutations in *mmpL3*; however, there is limited evidence that they are direct MmpL3 inhibitors. The lack of activity assays for MmpL3 made it impossible to test the proposed mechanism of action of these putative inhibitors.

Here, we report that MmpL3 is the TMM flippase at the IM. Using a spheroplast model, we developed assays to monitor IM topology of TMM. We found that 1,5-diarylpyrrole BM212 inhibits TMM flipping across the IM in wild-type spheroplasts. Furthermore, we established that specific MmpL3 variants confer resistance against this inhibition, indicating that MmpL3 is required for flipping TMM across the IM. BM212 does not inhibit the pmf or membrane potential, suggesting that it directly targets MmpL3. Our work represents the first demonstration of lipid transport activity of a key member of the MmpL protein family, and highlights the importance of using small molecule probes to interrogate protein function. Our assays have great utility in the validation and development of MmpL3-targeting small molecules as future anti-TB drugs.

Results

Spheroplasts serve as a viable system to monitor TMM topology

To develop a functional assay for TMM flipping across the IM, we sought a system where TMM topology in the IM can be monitored. Mycobacterial spheroplasts are ideal for this purpose because they lack the OM and cell wall, providing easy access to molecules-of-interest at the IM. Due to the loss of periplasmic contents upon the formation of spheroplasts, we also expect the transport pathway(s) for TMM to the OM to be disrupted, thereby resulting in accumulation of TMM at the IM. *M. smegmatis* spheroplasts were successfully generated via sequential treatment with glycine and lysozyme (Fig. S1), as previously reported (16). To examine whether MA synthesis is intact in spheroplasts, we profiled newly-synthesized lipids metabolically labeled with [^{14}C]-acetate. Thin layer chromatographic (TLC) analysis of lipids extracted from whole cells revealed two major species whose syntheses are inhibited by isoniazid, indicating that these are mycolate-based lipids (Fig. 1*B*). We assigned these species as TDM and TMM on the bases of reported retention factors of these lipids on TLC plates developed under the same solvent system (17). We showed that mycolates are still produced in *M. smegmatis* spheroplasts; however, the extracted lipids only contain TMM, but not TDM, consistent with the lack of TMM transport to the OM, where TDM synthesis occurs. Given the extreme hydrophobicity of mycolates, we conclude that newly-synthesized TMMs accumulate in the IM of spheroplasts, thus establishing a platform for monitoring TMM flipping across the bilayer.

TMMs accumulated in spheroplasts reside in the outer leaflet of the IM

We next examined whether newly-synthesized TMMs accumulated in the inner or outer leaflet of the IM in spheroplasts, by monitoring its accessibility to degradation by recombinant LysB, a lipolytic enzyme. LysB is a mycobacteriophage-encoded esterase that is specific for mycolates and plays the role of an endolysin important for the release of phage particles from infected cells (18,19). Substantial amounts of newly-synthesized TMMs in spheroplasts are readily and specifically hydrolyzed by purified LysB with the concomitant release of MAs (Fig. 2*A*). This suggests that newly-synthesized TMMs are accessible on the surface. We showed that an inactive LysB variant does not result in the same effect. In addition, we demonstrated that LysB does not enter spheroplasts, nor does it induce cell lysis compared to controls (Fig. 2*B*). Taken together, these results establish that the majority of newly-synthesized TMMs have been translocated across the IM in spheroplasts, and therefore reside in the outer leaflet of the membrane.

MmpL3 is responsible for flipping TMM across the IM

Several compounds, including SQ109, BM212 and AU1235, are believed to affect MmpL3-mediated TMM transport because mutations in *mmpL3* confer resistance against these small molecules (5,8,9). While it is not yet clear if these compounds directly inhibit MmpL3, they may be useful as probes to determine if MmpL3 is responsible for TMM flipping across the IM. Specifically, we asked whether these small molecules are able to inhibit TMM flipping in wild-type spheroplasts, and whether they would become less effective in doing so in spheroplasts expressing MmpL3 variants that confer resistance

against them. We first tested the effects of these compounds in our LysB assay in wild-type spheroplasts. Remarkably, BM212 and AU1235 are able to reduce LysB-mediated hydrolysis of newly-synthesized TMMs in *M. smegmatis* spheroplasts (Fig. 3*A* and *C*), at concentrations 2x and 4x above their reported minimal inhibitory concentrations (MICs) (Table S1) (5,9). In contrast, SQ109 has no effect (Fig. 3*B* and *C*). We showed that the effects of BM212 and AU1235 are not due to direct inhibition of LysB activity, since TMMs are still hydrolyzed in detergent-solubilized samples (Fig. S2). Instead, significant amounts of newly-synthesized TMMs are no longer accessible to LysB in the presence of either compound, indicating inhibition of TMM flipping across the IM. As an alternative method to assess TMM topology in the IM and the effects of these drugs, we also examined the ability of membrane-impermeable fluorophore-conjugated streptavidin to bind to newly-synthesized TMMs engineered to contain biotin (TMM-biotin) (Fig. 4*A*). Here, we metabolically labelled TMMs with 6-azido-trehalose (20), which allowed us to covalently attach an alkyne-containing biotin probe to TMM via the bio-orthogonal click reaction (21). In wild-type spheroplasts, TMM-biotin can be detected on the surface, indicating that 6-azido-TMMs have been translocated across the IM (Fig. 4*C*). We demonstrated that both BM212 and AU1235 drastically reduce the amounts of 6-azido-TMMs, and hence TMM-biotin, that can be labelled with streptavidin (Fig. 4*D* and *E*). Consistent with the LysB accessibility assay, these results establish that BM212 and AU1235 inhibit TMM flipping across the IM.

To establish whether MmpL3 is responsible for flipping TMM across the IM, we employed specific MmpL3 variants that render *M. smegmatis* cells less sensitive to BM212,

and tested if TMM flipping in spheroplasts expressing these variants would be more resistant to the effects of BM212. The growth of cells expressing MmpL3$_{V197M}$ or MmpL3$_{A326T}$ variants is only fully inhibited in the presence of 4-8 times the concentration of BM212 that inhibits wild-type growth (Table S1) (9). In wild-type spheroplasts, we showed that BM212 inhibits TMM flipping in a dose-dependent manner (Fig. 5*A* and *D*). We further demonstrated that BM212 is less effective at reducing LysB accessibility to TMM in spheroplasts expressing MmpL3$_{V197M}$ or MmpL3$_{A326T}$ variants (Fig. 5*B*, *C* and *D*). In fact, BM212 is also unable to inhibit the display of 6-azido TMMs on the surface of spheroplasts expressing MmpL3$_{V197M}$ (Fig. 5*E*, *F* and *G*). Since TMM is only accessible on the outer leaflet of the IM in the presence of functional MmpL3 (i.e. not inhibited by BM212), we conclude that MmpL3 is the TMM flippase.

BM212 directly inhibits MmpL3 function

MmpL3 function is believed to require the pmf, specifically the proton gradient (7). Consistently, we showed that proton gradient uncouplers, such as CCCP and nigericin (Fig. 3), but not membrane potential disruptors, such as valinomycin-K^+ (Fig. S3), can inhibit LysB accessibility to TMMs in spheroplasts. Whether BM212 inhibits TMM flipping by directly targeting MmpL3 is not clear. Contrary to previous reports (22), we did not observe effects on the proton gradient (Table S2) nor the membrane potential (Fig. S5) in spheroplasts treated with BM212, at concentrations that inhibited TMM flipping. Furthermore, mutations in *mmpL3* that confer resistance to BM212 cluster in a specific region when mapped onto a structural model of MmpL3 (Fig. 6), revealing a possible binding site. We therefore believe

188 that BM212 inhibits TMM flipping across the IM by binding MmpL3 directly.

189

190 **Discussion**

191 How the mycobacterial OM is assembled is not well understood. Many members of the
192 MmpL protein family are believed to be transporters that contribute to the assembly of
193 various OM lipids (23,24,25,26); however, their specific roles have not been clearly defined.
194 MmpL3 is the only member of this family essential for growth (5,6,7). Using two
195 independent assays that allow determination of TMM topology in the IM of mycobacterial
196 spheroplasts, and employing putative inhibitors as molecular probes to modulate protein
197 function, we have provided strong biochemical evidence that establish MmpL3 as the TMM
198 flippase. Whether MmpL3 is the only protein mediating TMM flipping, or whether it is also
199 involved in TMM release from the IM is not clear (Fig. 1*A*). One can posit that a second yet
200 identified protein may be necessary for extracting TMM from the IM and handing it to a
201 putative chaperone. This scenario would be comparable to the transport of lipoproteins across
202 the cell envelope in Gram-negative bacteria (27). Alternatively, this step may also be
203 mediated by MmpL3, in which case, flipping and release of TMM might be coupled; this
204 would suggest MmpL3 could interact with the putative chaperone. Extending from this idea,
205 a third scenario may be possible where TMM flipping and release are essentially one single
206 step in a mechanism similar to RND efflux pumps, whereby TMM never really resides in the
207 outer leaflet of the IM. This latter model is, however, less like since we have been able to
208 decouple these steps by observing TMM translocation across the IM in our spheroplasts,
209 which are effectively devoid of any putative chaperones. Moreover, despite being in the same

RND protein superfamily, the structure of MmpL3 differs substantially from canonical RND efflux pumps (28). MmpL3 does form trimers like RND pumps (29), but the periplasmic domains of MmpL3 are much smaller (28), and it contains a large C-terminal cytoplasmic domain. Therefore, MmpL3 may not export TMM via an efflux mechanism. Further characterization of this system would be necessary to tease apart these models.

TB is one of the leading causes of death by infectious disease, and remains a major health problem worldwide (30). With the rapid emergence of multi- and extensive-drug resistant (MDR/XDR) TB, there is an urgent need to develop anti-TB drugs with novel mechanisms-of-action. In this regard, drugs inhibiting MmpL3, which has been shown to be an ideal target (31), would be especially important. While many small molecules are thought to inhibit MmpL3, it is puzzling how molecules with different molecular scaffolds may bind and target the same protein. We have now developed assays that measure the topology of TMM in the IM of mycobacterial spheroplasts, allowing the validation of true MmpL3 inhibitors. As a start, we have established that BM212 directly inhibits MmpL3 function. Furthermore, we have shown that SQ109, a molecule that has reached (but failed) phase II clinical trials, does not actually inhibit TMM flipping. In fact, it is likely that many of these molecules do not inhibit MmpL3, and have other targets, as has been shown for tetrahydropyrazo[1,5-*a*]pyrimidine-3-carboxamides (32). Our assays will help to select and advance small molecules currently under development as MmpL3-targeting drugs.

Materials and Methods

Detailed methods can be found in *SI Appendix, Materials and Methods*.

Acknowledgments

We thank Graham Hatfull (U Pittsburgh) for providing the pLAM3 plasmid for LysB overexpression, and Derek Lin (NUS) for constructing the inactive $LysB_{S82A}$ variant. We are grateful to Benjamin Swarts (Central Michigan U) for his generous gift of 6-azido-trehalose. We also thank Eric Rubin (Harvard School of Public Health) for providing strains, and for critical discussion and comments on the manuscript. We acknowledge Jasmine Chen (Mechanobiology Institute) for help with microscopy. This work was supported by the National University of Singapore Start-up funding, the Singapore Ministry of Education Academic Research Fund Tier 1 and Tier 2 (MOE2014-T2-1-042) grants (to S.-S.C.).

244 **References**

1. Brennan, P. J. & Nikaido, H. (1995) The envelope of mycobacteria. *Annual Review of Biochemistry* 64(1):29-63.

2. Takayama, K., Wang, C. & Besra, G. S. (2005) Pathway to synthesis and processing of mycolic acids in Mycobacterium tuberculosis. *Clinical Microbiology Reviews* 18(1):81-101.

3. Banerjee, A. *et al.* (1994) inhA, a gene encoding a target for isoniazid and ethionamide in Mycobacterium tuberculosis. *Science* 263:227-229.

4. Jackson, M. *et al.* (1999) Inactivation of the antigen 85C gene profoundly affects the mycolate content and alters the permeability of the Mycobacterium tuberculosis cell envelope. *Molecular Microbiology* 31(5):1573-1587.

5. Grzegorzewicz, A. E. *et al.* (2012) Inhibition of mycolic acid transport across the Mycobacterium tuberculosis plasma membrane. *Nature Chemical Biology* 8(4):334-341.

6. Varela, C. *et al.* (2012) MmpL genes are associated with mycolic acid metabolism in mycobacteria and corynebacteria. *Chemistry & Biology* 19(4):498-506.

7. Domenech, P., Reed, M. B. & Barry, C. E. (2005) Contribution of the Mycobacterium tuberculosis MmpL protein family to virulence and drug resistance. *Infection and Immunity* 73(6):3492-3501.

8. Tahlan, K. *et al.* (2012) SQ109 targets MmpL3, a membrane transporter of trehalose monomycolate involved in mycolic acid donation to the cell wall core of Mycobacterium tuberculosis. *Antimicrobial Agents and Chemotherapy* 56(4):1797-1809.

9. La Rosa, V. *et al.* (2012) MmpL3 is the cellular target of the antitubercular pyrrole derivative BM212. *Antimicrobial Agents and Chemotherapy* 56(1):324-331.

10. Poce, G. *et al.* (2013) Improved BM212 MmpL3 inhibitor analogue shows efficacy in acute murine model of tuberculosis infection. *PLoS One* 8(2):e56980.

11. Stanley, S. A. *et al.* (2012) Identification of novel inhibitors of M. tuberculosis growth using whole cell based high-throughput screening. *ACS Chemical Biology* 7(8):1377-1384.

12. Remuiñán, M. J. *et al.* (2013) Tetrahydropyrazolo [1, 5-a] pyrimidine-3-carboxamide and N-benzyl-6′, 7′-dihydrospiro [piperidine-4, 4′-thieno [3, 2-c] pyran] analogues with bactericidal efficacy against Mycobacterium tuberculosis targeting MmpL3. *PLOS One* 8(4):e60933.

13. Rao, S. P. S. *et al.* (2013) Indolcarboxamide is a preclinical candidate for treating multidrug-resistant tuberculosis. *Science Translational Medicine* 5(214):214ra168.

14. Lun, S. *et al.* (2013) Indoleamides are active against drug-resistant Mycobacterium tuberculosis. *Nature Communications* 4:2907.

15. Dupont, C. *et al.* (2016) A new piperidinol derivative targeting mycolic acid transport in Mycobacterium abscessus. *Molecular Microbiology* 101(3):515-529.

16. Dhiman, R. K. *et al.* (2011) Lipoarabinomannan localization and abundance during growth of Mycobacterium smegmatis. *Journal of Bacteriology* 193(20):5802-5809.

17. Bansal-Mutalik, R. & Nikaido, H. (2014) Mycobacterial outer membrane is a lipid bilayer and the inner membrane is unusually rich in diacyl phosphatidylinositol dimannosides.

Proceedings of the National Academy of Sciences 111(13):4958-4963.

18. Payne, K. M. & Hatfull, G. F. (2012) Mycobacteriophage endolysins: diverse and modular enzymes with multiple catalytic activities. *PLoS One* 7(3):e34052.
19. Gil, F. *et al.* (2010) Mycobacteriophage Ms6 LysB specifically targets the outer membrane of Mycobacterium smegmatis. *Microbiology* 156(5):1497-1504.
20. Swarts, B. M. *et al.* (2012) Probing the mycobacterial trehalome with bioorthogonal chemistry. *Journal of the American Chemical Society* 134(39):16123-16126.
21. Jewett, J. C., Sletten, E. M. & Bertozzi, C. R. (2010) Rapid Cu-free click chemistry with readily synthesized biarylazacyclooctynones. *Journal of the American Chemical Society* 132(11):3688-3690.
22. Li, W. *et al.* (2014) Novel insights into the mechanism of inhibition of MmpL3, a target of multiple pharmacophores in Mycobacterium tuberculosis. *Antimicrobial Agents and Chemotherapy* 58(11):6413-6423.
23. Converse, S. E. *et al.* (2003) MmpL8 is required for sulfolipid-1 biosynthesis and Mycobacterium tuberculosis virulence. *Proceedings of the National Academy of Sciences* 100(10):6121-6126.
24. Jain, M. & Cox, J. S. (2005) Interaction between polyketide synthase and transporter suggests coupled synthesis and export of virulence lipid in M. tuberculosis. *PLoS Pathogen* 1(1):e2.
25. Pacheco, S. A., Hsu, F.-F., Powers, K. M. & Purdy, G. E. (2013) MmpL11 protein transports mycolic acid-containing lipids to the mycobacterial cell wall and contributes to

biofilm formation in Mycobacterium smegmatis. *Journal of Biological Chemistry* 288(33):24213-24222.

26. Belardinelli, J. M. *et al.* (2014) Biosynthesis and translocation of unsulfated acyltrehaloses in Mycobacterium tuberculosis. *Journal of Biological Chemistry* 289(40):27952-27965.
27. Okuda, S. & Tokuda, H. (2011) Lipoprotein sorting in bacteria. *Annual Review of Microbiology* 65:239-259.
28. Chim, N. *et al.* (2015) The Structure and interactions of periplasmic domains of crucial MmpL membrane proteins from Mycobacterium tuberculosis. *Chemistry & Biology* 22(8):1098-1107.
29. Belardinelli, J. M. *et al.* (2016) Structure--Function Profile of MmpL3, the Essential Mycolic Acid Transporter from Mycobacterium tuberculosis. *ACS Infectious Diseases* 2(10):702-713.
30. Global actions and investments fall far short of those needed to end the global TB epidemic: WHO report 2016. *World Health Organization, Geneva (WHO/HTM/TB/2016.13)*.
31. Li, W. *et al.* (2016) Therapeutic potential of the Mycobacterium tuberculosis mycolic acid transporter, MmpL3. *Antimicrobial Agents and Chemotherapy* 60(9):5198-5207.
32. Cox, J. A. G. *et al.* (2016) THPP target assignment reveals EchA6 as an essential fatty acid shuttle in mycobacteria. *Nature Microbiology* 1:15006.
33. Kelley, L. A., Mezulis, S., Yates, C. M., Wass, M. N. & Sternberg, M. J. E. (2015) The

Phyre2 web portal for protein modeling, prediction and analysis. *Nature Protocols* 10(6):845-858.

34. Payne, K., Sun, Q., Sacchettini, J. & Hatfull, G. F. (2009) Mycobacteriophage Lysin B is a novel mycolylarabinogalactan esterase. *Molecular Microbiology* 73(3):367-381.

35. Deidda, D. *et al.* (1998) Bactericidal activities of the pyrrole derivative BM212 against multidrug-resistant and intramacrophagic Mycobacterium tuberculosis strains. *Antimicrobial Agents and Chemotherapy* 42(11):3035-3037.

36. Ozkan, P. & Mutharasan, R. (2002) A rapid method for measuring intracellular pH using BCECF-AM. *Biochimica et Biophysica Acta* 1572(1):143-148.

37. Li, K. *et al.* (2014) Multitarget drug discovery for tuberculosis and other infectious diseases. *Journal of Medicinal Chemistry* 57(7):3126-3139.

38. Laemmli, U. K. (1970) Cleavage of structural proteins during the assembly of the head of bacteriophage T4. *Nature* 227:680-685.

246

247

248 **Figure Legends**

249

250 **Fig. 1.** TMM biosynthesis is intact in mycobacterial spheroplasts. (*A*) A schematic diagram
251 illustrating the processes important for MA transport across the cell envelope. Following
252 synthesis, TMMs must be flipped across the IM, released from the IM and then transported
253 across the periplasm (presumably via a chaperone). MmpL3 is implicated in TMM transport
254 at the IM, but its exact role has not been elucidated. At the OM, the Ag85 complex transfers
255 the mycolate chain from one TMM molecule to cell wall-linked arabinogalactan (AG)
256 polysaccharides, or to another TMM molecule to form trehalose dimycolate (TDM). Other
257 known lipid species found in the OM and IM are omitted for simplicity. PL, phospholipid. (*B*)
258 TLC analysis of newly-synthesized [^{14}C]-labelled lipids extracted from wild-type *M.*
259 *smegmatis* cells (WC) and spheroplasts (SP), visualized by phosphor imaging. Lipids were
260 radiolabelled in the presence or absence of isoniazid as indicated. The developing solvent
261 system comprises chloroform-methanol-water (30:8:1). PE, phosphatidylethanolamine; CL,
262 cardiolipin; PI, phosphatidylinositol; PIM, phosphatidylinositol mannoside.

263

264 **Fig. 2.** Newly-synthesized TMMs in mycobacterial spheroplasts are accessible to degradation
265 by LysB, indicating that these TMMs reside in the outer leaflet of the IM. (*A*) TLC analyses
266 of newly-synthesized [^{14}C]-labelled lipids extracted from *M. smegmatis* spheroplasts treated
267 with purified functional or non-functional (S82A) LysB. Lipids were resolved on TLCs
268 developed using solvent systems comprising either chloroform-methanol-water (30:8:1) (*left*)
269 or hexane-diethylether-acetic acid (70:30:1) (*right*), followed by visualization via phosphor

imaging. In addition to MA, treatment with functional LysB also resulted in the release of an unidentified apolar lipid, annotated with an asterisk (*). TAG, triacylglycerol. (*B*) α-GroEL2 and α-His immunoblot analyses of pellet and supernatant fractions obtained from sedimentation of *M. smegmatis* spheroplasts treated with functional or non-functional (S82A) LysB, indicating that LysB does not induce cell lysis.

Fig. 3. Anti-mycobacterial compounds, BM212 and AU1235, reduce TMM accessibility to LysB in spheroplasts, indicating inhibition of TMM flipping across the IM. (*A, B*) Representative TLC analyses of [^{14}C]-labelled lipids newly-synthesized in the presence of indicated concentrations of (*A*) BM212, AU1235, and (*B*) SQ109, and extracted from *M. smegmatis* spheroplasts following treatment with or without purified LysB. The effects of carbonyl cyanide *m*-chlorophenyl hydrazone (CCCP) and nigericin, which are known to disrupt the pmf, were also tested. At higher concentrations, these uncouplers affected lipid synthesis, consistent with the depletion of ATP. DMSO and methanol were used to dissolve the respective compounds and thus serve as negative controls. Equal amounts of radioactivity were spotted for each sample. The developing solvent system comprises chloroform-methanol-water (30:8:1). (*C*) A graphical plot showing the effects of various compounds on the amounts of TMMs remaining in spheroplasts following LysB treatment. TMM levels were quantified from TLCs shown in (*A*) and (*B*) expressed as a percentage of total mycolates (TMM+MA), and normalized against that in corresponding control samples without LysB treatment. Average normalized percentages and standard deviations from three

biological replicates are plotted. Student's t-test: *, $p < 0.05$ compared to the corresponding DMSO or methanol controls.

Fig. 4. Anti-mycobacterial compounds, BM212 and AU1235, reduce surface display of 6-azido-TMMs in spheroplasts, indicating inhibition of TMM flipping across the IM. (*A*) A schematic diagram illustrating the 6-azido-TMM surface display assay. Spheroplasts were incubated with 6-azido-trehalose to allow synthesis of 6-azido-TMM (20), which were subsequently labelled with alkyne-containing biotin (DIBO-biotin) via click chemistry (21). Surface-exposed TMM-biotin molecules were then recognized by Alexa Fluor 488-conjugated streptavidin, and visualized by fluorescence microscopy. (*B-E*) Representative bright-field and fluorescence microscopy images following DIBO-biotin/Alexa Fluor 488-streptavidin labelling of spheroplasts synthesizing (*B*) TMM, or 6-azido-TMM in the presence of (*C*) DMSO, (*D*) BM212 (2xMIC), and (*E*) AU1235 (2xMIC). Scale bars = 3 μm.

Fig. 5. Mutations in MmpL3 render BM212 less effective in the inhibition of TMM flipping across the IM. (*A-C*) Representative TLC analyses of [^{14}C]-labelled lipids newly-synthesized in the presence of indicated concentrations of BM212, and extracted from (*A*) WT, (*B*) *mmpL3*$_{V197M}$, and (*C*) *mmpL3*$_{A326T}$ *M. smegmatis* spheroplasts following treatment with or without purified LysB. DMSO serves as a negative control. Equal amounts of radioactivity were spotted for each sample. The developing solvent system comprises chloroform-methanol-water (30:8:1). (*D*) A graphical plot showing the dose-dependent

313 effects of BM212 on the amounts of TMMs remaining in the respective spheroplasts
314 following LysB treatment. TMM levels were quantified from TLCs shown in (*A*-*C*) expressed
315 as a percentage of total mycolates (TMM+MA), and normalized against that in corresponding
316 control samples without LysB treatment. Average normalized percentages and standard
317 deviations from three biological replicates are plotted. Student's t-test: *, $p < 0.05$; **, $p <$
318 0.01 compared to the corresponding DMSO controls for each respective strain. (*E*-*G*)
319 Representative bright-field and fluorescence microscopy images following
320 DIBO-biotin/Alexa Fluor 488-streptavidin labelling of *mmpL3*$_{V197M}$ spheroplasts synthesizing
321 (*E*) TMM, or 6-azido-TMM in the presence of (*F*) DMSO, and (*G*) BM212 (2xMIC). Scale
322 bars = 3 μm.
323
324 **Fig. 6.** Mutations that confer resistance against BM212 cluster on a structural model of
325 MmpL3, suggesting a possible binding site. A phyre2 (33) structural model for *M. smegmatis*
326 MmpL3 without its C-terminal cytoplasmic domain is shown in side- (*left*) and top-view
327 (*right*) orientations. For clarity, periplasmic domains are removed from the top-view
328 orientation. Residues important for passage of protons are highlighted in black. Residues that
329 conferred resistance against BM212 (9) when mutated in MmpL3 from *M. smegmatis*, *M.*
330 *bovis BCG* and *M. tuberculosis* are highlighted in red, purple and cyan, respectively.
331

Figures

Figure 1

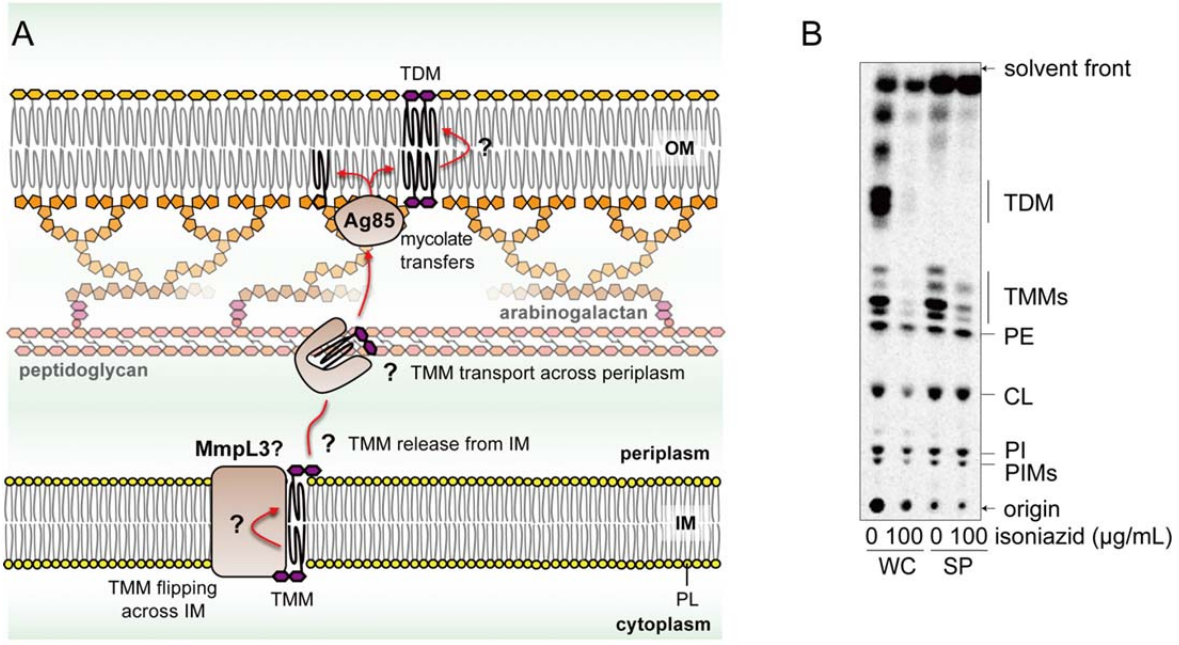

336 **Figure 2**

337

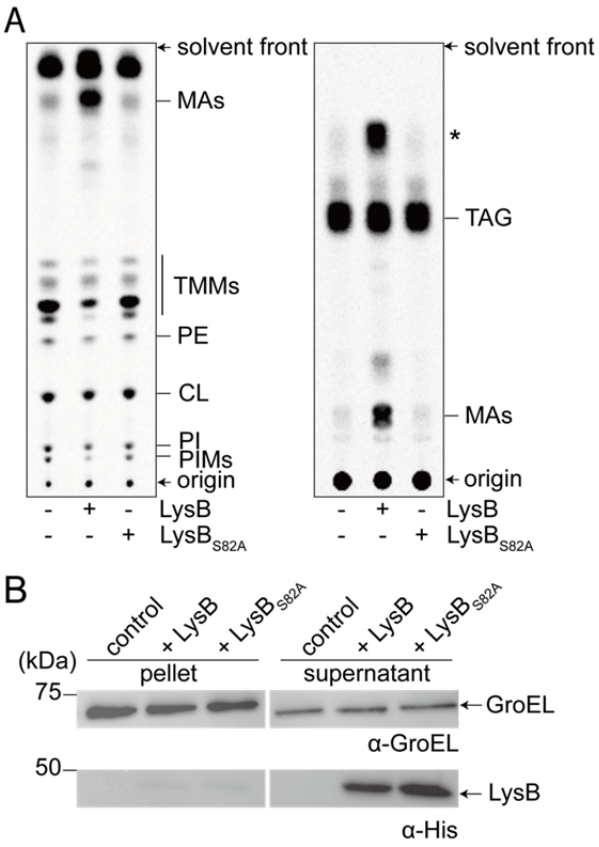

338

339

340 **Figure 3**

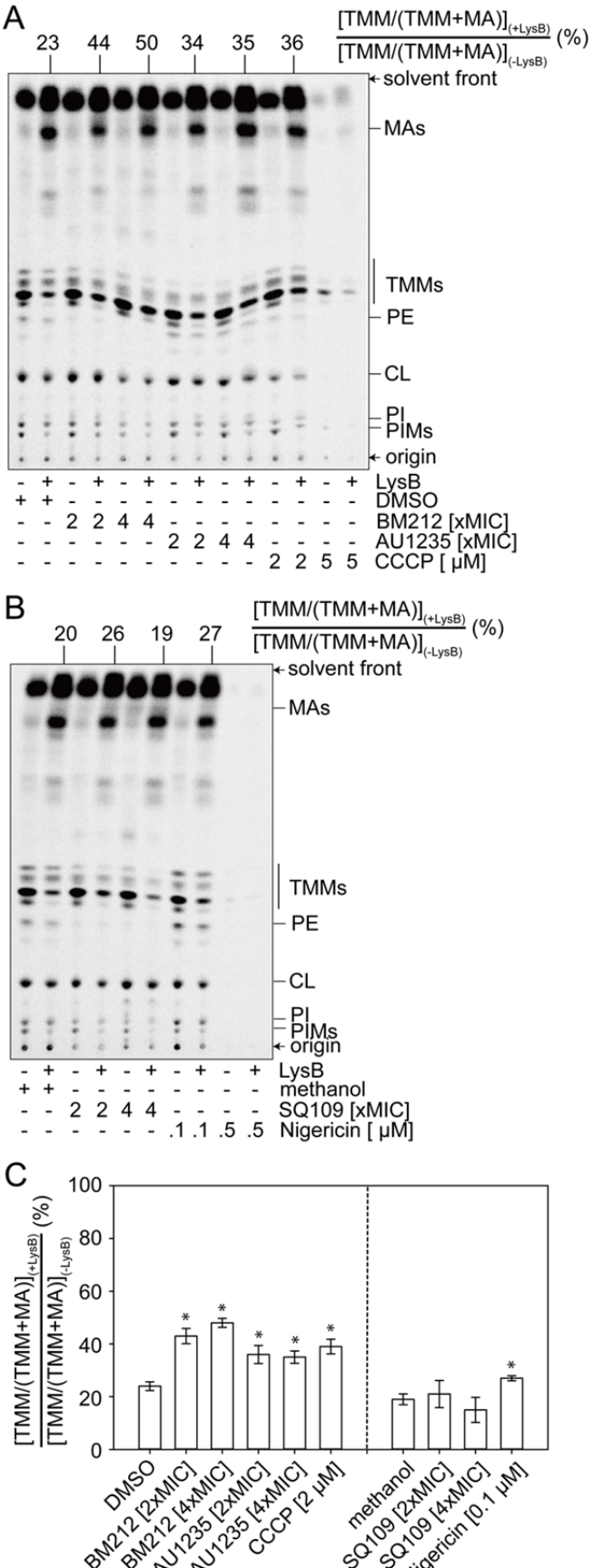

341

342 **Figure 4**

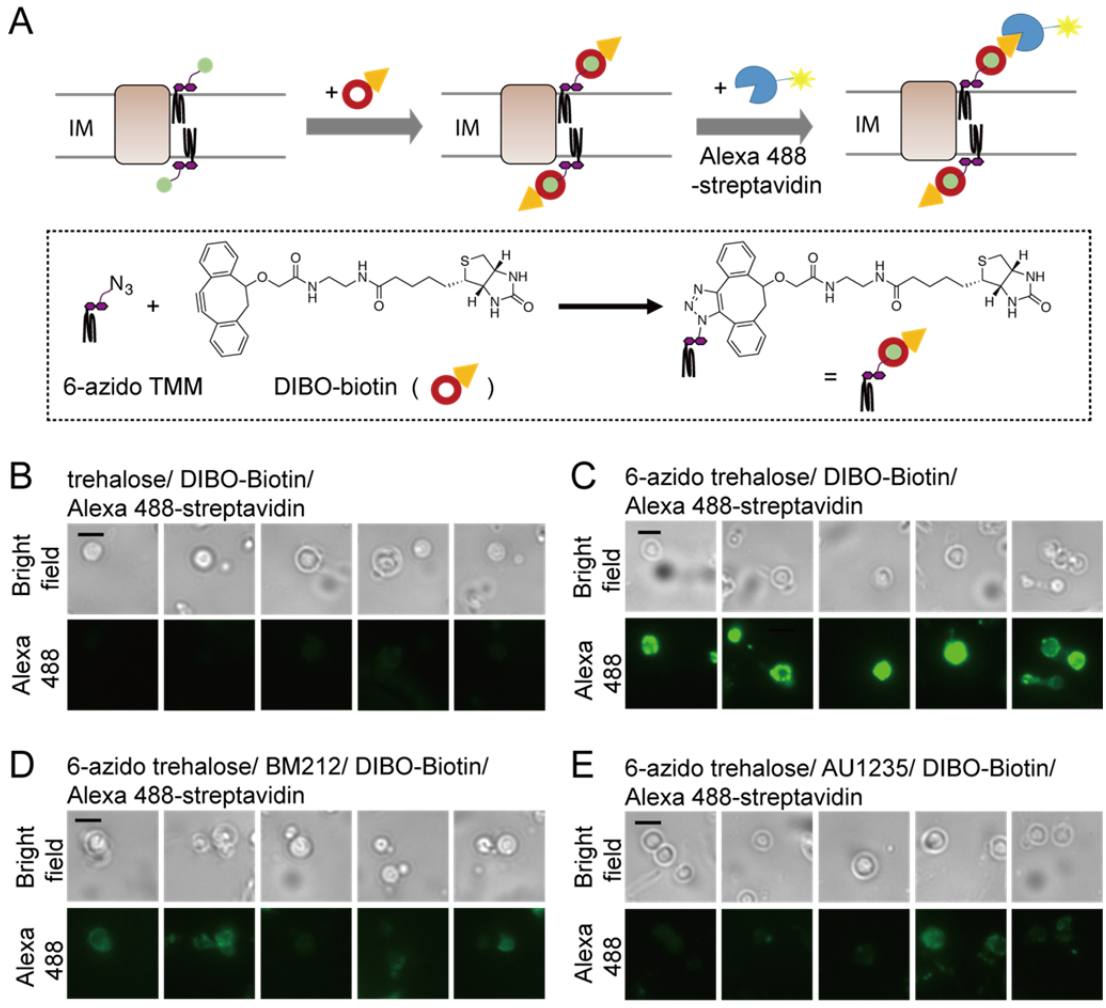

343

344

345 **Figure 5**

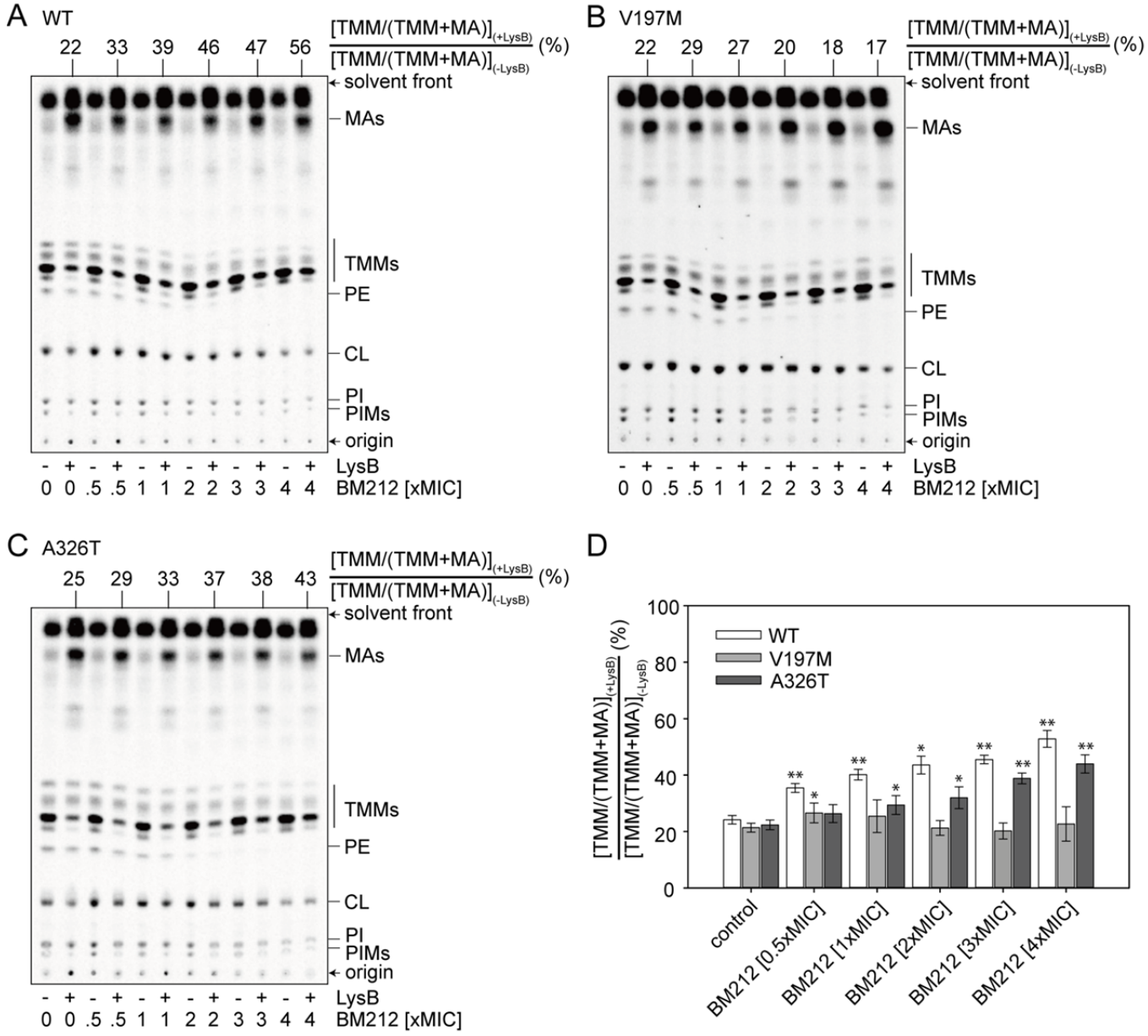

346

347 **Figure 6**

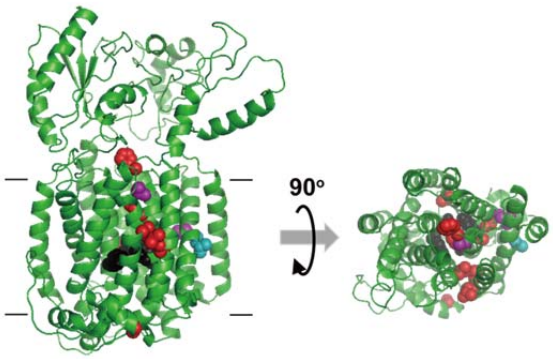

348

349

Supplementary Information

Title: MmpL3 is the flippase for mycolic acids in mycobacteria

Authors: Zhujun Xu[a], Giovanna Poce[c], Shu-Sin Chng[a,b,*]

Affiliations:

[a]Department of Chemistry, National University of Singapore, Singapore 117543.

[b]Singapore Center on Environmental Life Sciences Engineering (SCELSE), National University of Singapore, Singapore 117456.

[c]Dipartimento di Chimica e Tecnologie del Farmaco, Sapienza University of Rome, Rome 00185, Italy

[*]To whom correspondence should be addressed. E-mail: chmchngs@nus.edu.sg

Supplementary Materials and Methods

Bacterial strains and growth conditions. *M. smegmatis* mc^{2}155 was used in all experiments unless otherwise noted. BM212-resistant *M. smegmatis* strains, SRBM212_26 (*mmpL3*$_{V197M}$) and SRBM212_20 (*mmpL3*$_{A326T}$), were obtained from the Rubin laboratory at Harvard School of Public Health (9). For spheroplast formation, strains were grown in tryptic soy broth (TSB; BD Falcon) containing 1% glucose and 0.05% Tween 80 (16). For drug susceptibility tests, strains were grown in 7H9 broth (BD Falcon) containing 10% ADC enrichment (BD Falcon) and 0.05% Tween 80, or on 7H10 solid agar with 10% OADC enrichment (BD Falcon). *Escherichia coli* BL21(λDE3) was used for overexpression and purification of wild-type LysB and its non-functional LysB$_{S82A}$ variant from pLAM3 (pET24a(+)*lysB-His*) (34) and pET24a(+)*lysB*$_{S82A}$*-His*, respectively.

Chemicals. BM212 was synthesized as previously reported (35). BM212 and AU1235 (JS Research Chemicals Trading) were solubilized in DMSO at 1 mg/ml and used as stock solutions. SQ109 (Vector Biomed) was solubilized in methanol at 1 mg/ml. CCCP (Sigma-Aldrich) was prepared as a 1-mM stock solution in DMSO. Nigericin (Sigma-Aldrich) was prepared as a 2-mM stock solution in methanol. Valinomycin (Sigma-Aldrich) was prepared as a 3-mM stock solution in ethanol.

Spheroplast formation. *M. smegmatis* cells were converted to spheroplasts as described by Rakesh K et al (16). Briefly, a vial of *M. smegmatis* mc^{2}155 glycerol stock was thawed and

387 inoculated into TSB with 1% glucose and 0.05% Tween 80, followed by incubation at 37°C
388 and 180 rpm until the optical density (OD_{600}) reached ~1.0. Glycine was then added into the
389 culture to a final concentration of 1.2% (w/v), followed by continued incubation at 37°C and
390 120 rpm for 20 to 24 h. The glycine-treated cells were harvested by centrifugation at 4,000 x
391 *g*, washed with 1xSMM buffer (final pH 6.8; 0.5 M sucrose and 20 mM $MgCl_2$ in 20 mM
392 maleate buffer at pH 6.6), and re-suspended in TSB-SMM (TSB containing 1xSMM buffer)
393 by gentle pipetting. Filter-sterilized solutions of lysozyme (5 mg/ml) and glycine (20% (w/v))
394 were added to final concentrations of 50 µg/ml and 1.2% (w/v), respectively. Spheroplast
395 formation was complete after incubation at 37°C and 120 rpm for another 20 to 24 h. The
396 final mixture was washed with 1xSMM buffer and filtered through a sterile cell strainer (20
397 µm; BD Falcon) to eliminate clumps of cells. The successful generation of *M. smegmatis*
398 spheroplasts was confirmed by examining morphology changes in both bright-field and
399 fluorescence (DAPI, FM14-3) images taken using an Olympus IX71 inverted microscope.
400
401 **Lipid profiling of *M. smegmatis* spheroplasts.** To label all lipids, *M. smegmatis* mc^2155
402 cells or spheroplasts (OD_{600} = 0.8) were incubated for 2 h at 37˚C in TSB or TSB-SMM (pH
403 6.8), respectively, containing sodium [1-^{14}C]-acetate (final concentration 0.2 µCi/ml; Perkin
404 Elmer NEC084A001MC). Where indicated, 100 µg/ml isoniazid (Sigma-Aldrich) was added
405 to inhibit mycolic acid synthesis prior to [^{14}C]-labelling. Labelled cells or spheroplasts were
406 harvested by centrifugation at 5,000 x *g* for 10 min, and lipids extracted as follows. Briefly,
407 cell pellets (from 1-ml cultures at OD_{600} = 0.8) were resuspended in 800-µl of single-phase
408 chloroform-methanol-water (2:1:0.2) solution, followed by three repeats of alternating bath

409 sonication (1 min duration) and brief vortexing. Appropriate volumes of methanol and water
410 were then added to give a two-phase chloroform-methanol-water (1:1:0.8) mixture, the
411 sample vortexed, and then centrifuged at 10,000 x *g* for 5 min to achieve phase separation.
412 The organic phases (bottom phase) containing lipids were collected and air-dried overnight in
413 a fumehood. Lipids were analyzed by TLC, and visualized by phosphor imaging.
414
415 **Assessing TMM accessibility to degradation in spheroplasts by purified LysB.** To label
416 all lipids, *M. smegmatis* mc^2155 spheroplasts (OD_{600} = 0.8) were incubated for 2 h at 37˚C in
417 1xSMM buffer (pH 6.8) containing sodium [1-^{14}C]-acetate (final concentration 0.2 µCi/ml;
418 Perkin Elmer NEC084A001MC). Following labelling, 1-ml spheroplast suspensions were
419 aliquoted into separate microcentrifuge tubes and treated with purified LysB (50 µg/ml final
420 concentration), purified inactive $LysB_{S82A}$, or no LysB for 30 min at 37˚C. Treated
421 spheroplasts were harvested by centrifugation at 5,000 x *g* for 10 min. Lipids were extracted
422 according to the procedure outlined in the "Lipid profiling" section, analyzed by TLC, and
423 visualized by phosphor imaging. To test the effects of putative MmpL3 inhibitors in this assay,
424 spheroplasts were pre-treated (prior to labelling) with indicated concentrations of compounds,
425 including BM212, AU1235, SQ109 and valinomycin (in presence of 100 mM KCl), and
426 incubated for 15 min at 37˚C. DMSO, methanol and ethanol were used as negative controls
427 (depending on the solvent used to solubilize each compound), while CCCP and nigericin
428 were used as positive controls.
429 To examine if selected compounds (BM212 and AU1235) affected the activity of
430 LysB, samples were treated with DDM (final concentration 0.02% (w/v)) to lyse spheroplasts

after radiolabeling and prior to LysB treatment. Following LysB treatment, lipids were extracted from the whole solution with a slightly modified procedure. Appropriate volumes of chloroform and methanol were added to the ~1-ml solution to give a single-phase chloroform-methanol-water (1:2:0.8) solution. The sample was then subjected to five repeats of alternating bath sonication (2 min duration) and brief vortexing (10 s). The final solution was converted to a two-phase chloroform-methanol-water (1:1:0.8) mixture by adding appropriate volumes of chloroform and water, vortexed and finally centrifuged at 4,000 x *g* for 30 min to achieve phase separation. The organic phases (bottom phase) containing lipids were collected and air-dried overnight in a fumehood. Lipids were analyzed by TLC, and visualized by phosphor imaging.

To test if treatment with LysB resulted in lysis of spheroplasts, mock reactions not containing radioactive sodium acetate were set up so as to examine cytoplasmic protein localization after cell fractionation. *M. smegmatis* mc^2155 spheroplasts (OD_{600} = 0.8) were incubated for 2 h at 37˚C in 1xSMM buffer (pH 6.8) containing sodium acetate (final concentration 18 µg/ml). 1-ml spheroplast suspensions were then aliquoted into separate microcentrifuge tubes and treated with purified LysB (50 µg/ml final concentration), purified inactive $LysB_{S82A}$, or no LysB for 30 min at 37˚C. Treated spheroplasts were centrifuged at 5,000 x *g* for 10 min to separate cell pellets and supernatants. Pellets were washed twice and resuspended in 1-ml 1xSMM buffer. Supernatants were further purified by two sequential centrifugation steps (10,000 x *g*, 10 min) to remove residual spheroplasts. 100 µl from both pellet and supernatant samples were mixed separately with equal volumes of 2x Laemmli SDS-PAGE reducing sample buffer, and boiled at 100°C for 10 min. Equal volumes of all

453 samples were then subjected to SDS-PAGE, followed by immunoblotting using antibodies
454 against GroEL2 (cytoplasmic protein) and the penta-histidine tag (to detect LysB-His).
455
456 **Thin layer chromatography.** All dried radiolabeled lipid samples were suspended in 100 µl
457 chloroform-methanol (4:1). Equal volumes (20 µl) of samples were mixed with 2 ml of
458 Ultima Gold scintillation fluid (Perkin Elmer, Singapore). The [^{14}C]-counts were measured
459 using scintillation counting (MicroBeta2®, Perkin-Elmer) and taken as the levels of total
460 lipids isolated from the spheroplasts. Equal amounts (~5,000 cpm) of radioactivity were
461 spotted on Silica 60 F_{254} TLC plates (Merck). TLCs were developed in chambers
462 pre-equilibrated for 30 min with solvent systems chloroform-methanol-water (30:8:1) or
463 hexane-diethylether-acetic acid (70:30:1), where indicated. After development, TLC plates
464 were air-dried for 2 hours and later visualized by phosphor imaging (STORM, GE healthcare).
465 Densitometric analyses of TMM and MA spots for each lane (sample) on the phosphor
466 images of TLCs were carried out using ImageQuant TL analysis software (version 7.0, GE
467 Healthcare).
468
469 **Overexpression and purification of D29 mycobacteriophage LysB and its inactive**
470 **variant.** BL21(λDE3) containing pLAM3 (pET24a(+)*lysB-His*) (34) or
471 pET24a(+)*lysB*$_{S82A}$*-His* were used for overexpression and purification of wild-type LysB or
472 its non-functional $LysB_{S82A}$ variant, respectively. pLAM3 was a kind gift from Graham
473 Hatfull (University of Pittsburgh). pET24a(+)*lysB*$_{S82A}$*-His* was constructed from pLAM3 via
474 site-directed mutagenesis. For each strain, 30-ml small culture was first grown from single

colony in LB broth (supplemented with 200 µg/ml ampicillin) at 37°C until OD_{600} ~0.5-0.7. A 3-l culture was then inoculated using the small culture at 1:100 dilution and grown in LB broth at 37°C until OD_{600} ~0.5-0.7. Isopropyl β-D-1-thiogalactopyranoside (IPTG; 1st Base) was subsequently added to large cultures to get a final concentration of 1 mM. After incubation at 37°C for 2 h, cells were harvested by centrifugation at 4,700 x *g* for 20 min. Pelleted cells were resuspended in 20 ml of cold buffer A (20 mM Tris HCl, pH 8.0, 150 mM NaCl) containing 100 µg/ml lysozyme, 100 µM phenylmethylsulfonyl fluoride (PMSF) and 50 µg/ml DNase I. The re-suspended cells were lysed by a single passage through a high pressure French Press (French Press G-M, Glen Mills) homogenizer at 20,000 psi. Unbroken cells were removed by centrifugation at 5,000 x *g* for 10 min. The cell lysate was collected and centrifuged at 100,000 x *g* for 1 h in an ultracentrifuge (Model XL-90, Beckman Coulter) to remove membrane debris. The supernatant was collected, loaded onto a column packed with 2.5 mL of TALON cobalt resin (Clontech) pre-equilibrated with 25 mL of buffer B (50 mM Tris HCl, 300 mM NaCl, 10 mM imidazole, pH 8.0), and incubated at 4°C for 1 h with rocking. The resin mixture was later allowed to drain by gravity. The filtrate was collected, reloaded into the column and drained as above. The resin was washed with 4 x 25 ml buffer B, and then eluted with 10 ml of buffer C (50 mM Tris HCl, 150 mM NaCl, 200 mM imidazole, pH 8.0). The eluate was concentrated in a 10 kDa cut-off ultra-filtration device (Amicon Ultra, Merck Millipore) by centrifugation at 4,000 x *g* to ~250 µl. The concentrated samples were further purified by size exclusive chromatography on an AKTA Pure machine using a prepacked Superdex 75 column (GE Healthcare) with TBS as the eluent. The concentrations of purified LysB and $LysB_{S82A}$ were determined using the DC™ protein assay

(Bio-Rad).

6-azido-TMM surface display assay. 1-ml of *M. smegmatis* spheroplasts (OD = 0.8) in 1xSMM buffer was fed with 100 μM 6-azido-trehalose (a kind gift of Benjamin Swarts (Central Michigan U)) at 37˚C for 2 h to allow the biosynthesis of 6-azido-TMM (20). The same concentration of trehalose was employed for spheroplasts used as a negative control. Spheroplasts were washed twice with 1xSMM buffer, resuspended in 1 ml of the same buffer, and then incubated at room temperature with Click-IT® Biotin DIBO Alkyne (final 5 μg/ml; ThermoFisher Scientific product no. C10412) for 1 hour in the dark. This step labels all 6-azido-TMMs via click chemistry to afford biotin-TMMs. Following this, spheroplasts were again washed thrice with 1xSMM buffer and resuspended in 1 ml of the same buffer. To specifically label surface-exposed biotin-TMMs, Alexa Fluor® 488 streptavidin (final 1 μg/ml; ThermoFisher Scientific product no. S32354) was added to the spheroplasts and incubated for 1 hour at room temperature in the dark. Following three washes with 1xSMM buffer, the spheroplasts were re-suspended in 50 μl 1xSMM buffer. 10 μl of each sample was spotted onto a microscope glass slide. Bright-field and fluorescence (λ_{ex} 488 nm/ λ_{em} 525 nm) images were captured on an Olympus IX71 inverted microscope using an Photometrics CoolSNAP HQ^2 camera and SoftWoRx 4.10 software (MBI NUS). To test the effects of putative MmpL3 inhibitors in this assay, spheroplasts were pre-treated (prior to labelling with 6-azido-trehalose) with indicated concentrations of compounds, including BM212 and AU1235, and incubated for 15 min at 37˚C. In addition, all wash buffers contained the same concentrations of these compounds. DMSO was used as a negative control.

Determination of intracellular pH using the 2',7'-bis-(2-carboxyethyl)-5-(and-6)-carboxyfluorescein acetoxymethyl ester (BCECF-AM) dye. The effects of inhibitors on ΔpH were determined using BCECF, a pH-sensitive fluorescent dye activated inside cells via esterase-mediated hydrolysis of BCECF-AM (36). First, a standard curve was generated as follows. Briefly, *M. smegmatis* spheroplasts (OD = 0.8) in 1xSMM buffers at various pHs (6.0 - 8.0) were incubated with 20 μM BCECF-AM at 37˚C for 30 min in the presence of 20 μM nigericin. Nigericin is a proton uncoupler and serves to allow equilibration of protons (pH) across the membrane. The buffers also contained 100 mM potassium chloride (KCl), presumably to ensure a steady membrane potential (Δψ). Fluorescence emission (λ_{em} 525 nm) intensities of intracellular BCECF were measured following excitation at λ_{ex} 488 and 440 nm in a SPECTRAmax 250 microplate spectrophotometer equipped with SOFTmax PRO software (Molecular Devices). The ratio of fluorescence emission intensities at these two excitation wavelengths, or the fluorescence excitation profile (λ_{ex} 488 nm/λ_{ex} 440 nm), is pH-dependent. Average (λ_{ex} 488 nm/λ_{ex} 440 nm) values were obtained from technical triplicates and plotted against pH to obtain a linear standard curve (Extended Data Fig. 6).

To test the effects of putative MmpL3 inhibitors on intracellular pH (and hence ΔpH), spheroplasts (OD = 0.8) in 1xSMM buffer at pH 6.8 were pre-treated with indicated concentrations of compounds, including BM212, AU1235 and SQ109, and incubated at 37˚C for 30 min. DMSO and methanol were used as negative controls, while CCCP and nigericin were used as positive controls. 20 μM BCECF-AM was then added to the samples and

incubation was continued for 30 min before fluorescence measurements. Fluorescence excitation profiles (λ_{ex} 488 nm/λ_{ex} 440 nm) of BCECF for each condition were averaged (across three technical replicates) and calibrated against the standard curve. The intracellular pH and ΔpH are tabulated in Extended Data Table 2.

Membrane potential measurements in *M. smegmatis* spheroplasts. The effects of inhibitors on Δψ were determined using the membrane potential-sensitive 3,3'-dipropylthiodicarbocyanine ($DiSC_3(5)$) dye (37). $DiSC_3(5)$ binds to energized membranes and becomes quenched. When Δψ is disrupted, the dye leaves the membrane, resulting in an increase in fluorescence. 1.5-ml *M. smegmatis* spheroplasts (OD =0.8) were used in 1xSMM buffer containing 10 mM glucose and 1 μM nigericin (added to remove the effects of ΔpH). $DiSC_3(5)$ was then added to samples to get a final concentration of 5 μM and equilibrated for 10 min at room temperature. From this point, fluorescence was continuously monitored with a SPECTRAmax 250 microplate spectrophotometer equipped with SOFTmax PRO software (Molecular Devices), employing an excitation wavelength of 643 nm and an emission wavelength of 666 nm. The effects of various compounds, including BM212 and AU1235, on Δψ were measured by monitoring increase in fluorescence when these compounds were added at specific time points at indicated concentrations. DMSO and valinomycin (with potassium chloride) were used as positive and negative controls, respectively.

Drug susceptibility tests. MICs of compounds against various *M. smegmatis* strains were

563 determined using both solid and liquid media (10). For assays performed with solid media,
564 7H10 agar medium supplemented with 10% OADC and 0.5% glycerol was used to prepare
565 plates containing 2-fold serial dilutions of indicated compounds at concentrations ranging
566 from 0.78 to 50 μg/ml. Cell cultures were grown to mid-log growth phase (OD ~0.5-0.8) in
567 7H9 broth and diluted to a final concentration of ~2×10^6 cells/ml. One microliter of the
568 diluted culture was then streaked onto each plate and incubated at 37°C for 3 to 4 days. The
569 MIC was defined as the lowest concentration of compound that prevented the formation of
570 colonies.

571 For assays performed with liquid media, the MIC was defined as the lowest
572 concentration of compound that inhibited growth. Mycobacteria was inoculated at an OD_{600}
573 of 0.003 in wells with 200 μl 7H9 media containing 2-fold serial dilutions of indicated
574 compounds at concentrations ranging from 0.78 to 50 μg/ml, and incubated at 37°C for 24 h.
575 50 μl of a 1 mg/ml solution of MTT (Thiazolyl Blue Tetrazolium Bromide, Sigma) in sterile
576 water was added to each well. Samples were then incubated at room temperature for 2 hours
577 and color changes reflecting active metabolism (live cells) were monitored.

578

579 **SDS-PAGE and Western blots.** SDS-PAGE was performed according to Laemmli using the
580 4-12% Tris.HCl polyacrylamide gels (38). Immunoblotting was performed by transferring
581 protein bands from SDS-PAGE gels onto polyvinylidene fluoride (PVDF) membranes
582 (Immun-Blot® 0.2 μm, Bio-Rad) using the semi-dry electroblotting system (Trans-Blot®
583 TurboTM Transfer System, Bio-Rad). Membranes were blocked by 1x casein blocking buffer
584 (Sigma). α-His antibody (penta-histidine) conjugated to the horseradish peroxidase (HRP)

585 (Qiagen) was used at a dilution of 1:5,000. Mouse monoclonal α-GroEL2 antibody (BEI
586 Resources) was used at 1:1,000 dilution. Sheep α-mouse IgG secondary antibody conjugated
587 to HRP (GE Healthcare) was used at 1:5,000 dilution. Luminata Forte Western HRP Substrate
588 (Merck Milipore) was used and chemiluminescent signals were visualized using the G:BOX
589 Chemi XT 4 (Genesys version 1.3.4.0, Syngene).

590 **Supplementary Figure Legends**

591

592 **Fig. S1 M. smegmatis spheroplasts are successfully generated after treatment with**
593 **glycine and lysozyme.** Cellular morphologies of *M. smegmatis* cells and spheroplasts
594 visualized by light and fluorescence microscopy after labelling with membrane and DNA
595 dyes, FM14-3 and DAPI, respectively. Scale bar = 3 μm.

596

597 **Fig. S2 BM212 and AU1235 do not affect the activity of LysB.** Representative TLC
598 analysis of [^{14}C]-labelled lipids newly-synthesized in the presence of indicated concentrations
599 of BM212 and AU1235, and extracted from *M. smegmatis* spheroplasts following treatment
600 with or without purified LysB. Where indicated, n-dodecyl-β-maltoside (DDM) was added to
601 solubilize spheroplasts immediately prior to LysB addition. DMSO was used to dissolve the
602 compounds and thus serve as negative controls. Equal amounts of radioactivity were spotted
603 for each sample. The developing solvent system comprises chloroform-methanol-water
604 (30:8:1). TMM levels in samples with LysB treatment were quantified from the TLC,
605 expressed as a percentage of total mycolates (TMM+MA), and normalized against that in
606 corresponding control samples without LysB treatment. FA, fatty acid.

607

608 **Fig. S3 Membrane potential (Δψ) is not required for TMM flipping across the IM.**
609 Representative TLC analysis of [^{14}C]-labelled lipids newly-synthesized in the presence of
610 increasing concentrations of valinomycin (a potassium ionophore), and extracted from *M.*
611 *smegmatis* spheroplasts following treatment with or without purified LysB. Ethanol was used

612 to dissolve valinomycin and thus serve as a negative control. Equal amounts of radioactivity
613 were spotted for each sample. The developing solvent system comprises
614 chloroform-methanol-water (30:8:1). TMM levels in samples with LysB treatment were
615 quantified from the TLC, expressed as a percentage of total mycolates (TMM+MA), and
616 normalized against that in corresponding control samples without LysB treatment.
617
618 **Fig. S4 Standard curve for intracellular pH measurements using the BCECF dye** (36)**.**
619 The non-fluorescent BCECF acetoxymethyl ester (BCECF-AM) dye is used to measure
620 intracellular pH. Upon entering spheroplasts, BCECF-AM is hydrolyzed by esterases to
621 liberate BCECF, which is now fluorescent. The fluorescence excitation profile (λ_{ex} 488
622 nm/λ_{ex} 440 nm) of BCECF is pH-dependent and varies linearly in the range of pH 6 to 8.
623 Average (λ_{ex} 488 nm/λ_{ex} 440 nm) values and standard deviations from technical triplicates are
624 plotted.
625
626 **Fig. S5 BM212 and AU1235 have minimal effects on the membrane potential (Δψ) in *M.***
627 ***smegmatis* spheroplasts.** Fluorescence intensity changes of 3,3'-dipropylthiadicarbocyanine
628 iodide ($DiSC_3(5)$) dye in spheroplasts upon the addition of specified concentrations of
629 BM212 and AU1235 at the indicated time points. $DiSC_3(5)$ binds to energized membranes
630 and becomes quenched. When Δψ is disrupted, the dye leaves the membrane, resulting in an
631 increase in fluorescence. Valinomycin-K^+ and DMSO serve as positive and negative controls,
632 respectively.
633

Supplementary Figures

Figure S1

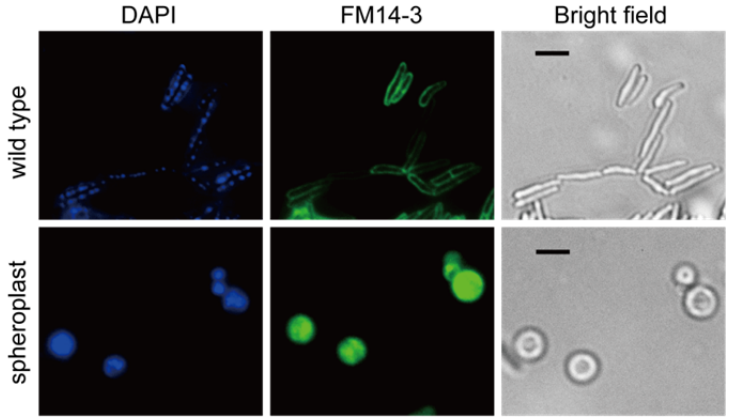

638 **Figure S2**

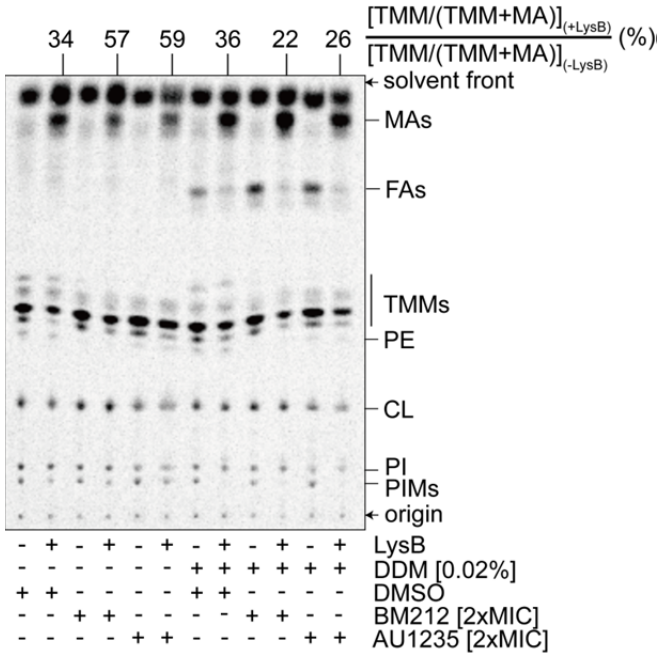

639

640

641 **Figure S3**

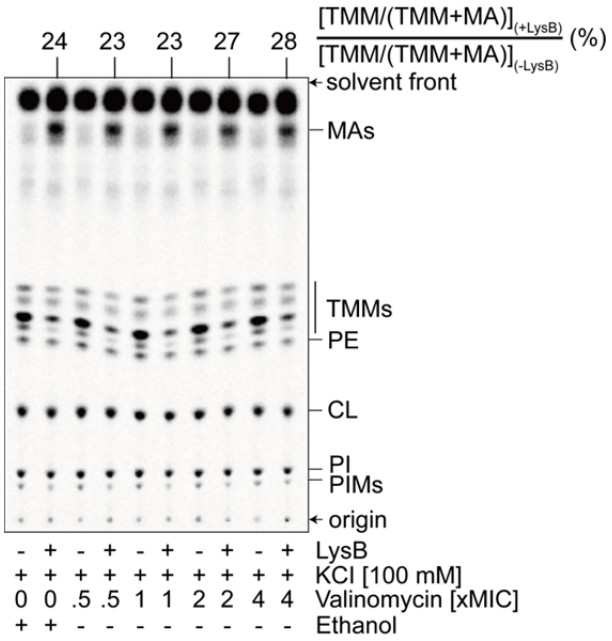

642

643

644 **Figure S4**

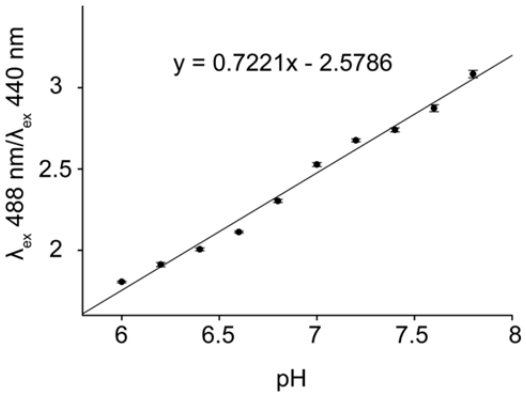

645

646

647 **Figure S5**

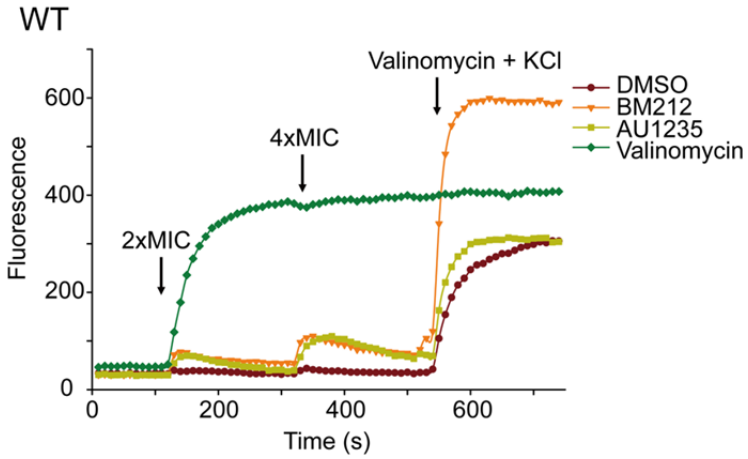

648

649 **Supplementary Tables**

650

651 **Table S1. Reported and measured minimal inhibitory concentrations (MICs) of various**
652 **compounds against indicated *M. smegmatis* strains.**

Strain	MIC (μg/ml)							
	BM212			AU1235			SQ109	
	reported	liquid	solid	reported	liquid	solid	reported	liquid
WT	3.125	3.125	3.125	3.125	3.125	3.125	3.125	3.125
mmpL3$_{V197M}$	25	12.5	12.5	-	-	-	-	-
mmpL3$_{A326T}$	25	12.5	12.5	-	-	-	-	-

653

654

Table S2. BM212, AU1235 and SQ109 do not affect the ΔpH across the IM in *M. smegmatis* spheroplasts.

Drug	$pH_{outside}$ *	pH_{inside} †	ΔpH ‡
DMSO	6.80	7.21 (±0.02)	0.41 (±0.02)
BM212 (2xMIC)	6.80	7.12 (±0.02)	0.32 (±0.02)
BM212 (4xMIC)	6.80	7.25 (±0.06)	0.45 (±0.06)
AU1235 (2xMIC)	6.80	7.11 (±0.02)	0.31 (±0.02)
AU1235 (4xMIC)	6.80	7.06 (±0.01)	0.26 (±0.01)
2 μM CCCP	6.80	6.74 (±0.01)	-0.06 (±0.01)
5 μM CCCP	6.80	6.65 (±0.02)	-0.15 (±0.02)
methanol	6.80	7.08 (±0.03)	0.28 (±0.03)
SQ109 (2xMIC)	6.80	7.47 (±0.28)	0.67 (±0.28)
SQ109 (4xMIC)	6.80	7.28 (±0.01)	0.48 (±0.01)
0.1 μM Nigericin	6.80	7.18 (±0.02)	0.38 (±0.02)
0.5 μM Nigericin	6.80	6.89 (±0.02)	0.09 (±0.02)

* refers to pH of external buffer.

† intracellular pH obtained using the 2',7'-bis-(2-carboxyethyl)-5-(and-6)-carboxyfluorescein (BCECF) dye. Measurements of the fluorescence excitation profile (λ_{ex} 488 nm/λ_{ex} 440 nm) of BCECF were averaged (across the three technical replicates) and calibrated against a standard curve (Supplementary Fig. 4). Standard deviations are given in parenthesis.

‡ pH_{inside} - $pH_{outside}$.